Manaaki Whenua
Landcare Research

Hyperspectral Signature of cLSO Infection of Seed Potatoes - a Shadehouse Experiment

Prepared for: Potatoes NZ

September 2019

Hyperspectral Signature of cLSO Infection of Seed Potatoes - a Shadehouse Experiment

Contract Report: LC[Editor will add]

Andrew M.S. McMillan

Manaaki Whenua – Landcare Research

Reviewed by:	*Approved for release by:*
Pierre Roudier Research Scientist Manaaki Whenua – Landcare Research	…

Contents

Summary 1
1 Introduction 2
2 Background 2
3 Objectives 3
4 Methods 4
5 Results 10
6 Conclusions 18
7 Recommendations 18
8 Acknowledgements 18
9 References 20

Appendix 1 21

Summary

Project and Client

- Project: Improving the quality of seed potatoes using precision agriculture – A Sustainable Farming Fund (SFF) Project
- Client: Potatoes NZ – Lead contractor for the SSF Project.

Objectives

- Investigate whether the CLso symptoms can be detected using hyperspectral imaging of the foliage of CLso-infected and uninfected potato plants

Methods

- Experiment 1. Infected (n=10) and healthy (n=10) Russel Burbank tubers were planted and grown in pots in a shadehouse at Lincoln on 23 October 2018.
    - Close-range (92 cm) hyperspectral imagery was collected for each plant on five occasions at 31, 35, 38, 48 and 52 days following planting.
- Experiment 2. Healthy tubers of Russel Burbank (n=20) and Innovator (n=20) were grown in pots. They were planted on 21 October 2019. On 23 January 2019 half of the plants in each cultivar group were infected with CLso via the Potato Psyllid vector.
    - Close-range hyperspectral imagery was collected for each plant on 10 occasions at beginning one day before infection and ending 54 days after infection (95 to 150 days following planting).
- Raw hyperspectral imagery (HSI) was converted to reflectance using Headwall Photonic's SpectralView software, and customised Python and R scripts were used to assess differences between infected and uninfected plants.

Results

- Experiment 1: Detecting CLso in plants from infected tubers
    - Variability in the spectra among replicate plants was of similar magnitude to differences between healthy and infected plants. This prevented CLso-detection that is purely based on the shape of the spectra.
    - However, we found significant differences between healthy and infected plants in the amount of leaf area with NDVI values between 0.8 to 0.9 at 30 days following planting.
- Experiment 2: Detecting CLso in plants infected with CLso via transmission from potato psyllids.
    - Spectral analysis, rather than the NDVI-class Green Area approach used in Experiment 1, was the preferred method of detecting CLso transmitted by psyllids.
    - There were marked differences in the spectral reflectance between infected and non-infected plants, and between the two cultivars tested. Infected plants

tended to be higher in the visible region from 570-650 nm and in the near-infrared region between 730 and 930 nm These differences provided the basis for early detection of CLso but further work is required to determine how this benchtop experiment could be translated to operational field conditions.

Conclusions

- Early stage tuber-transmitted CLso-infection was detected by measuring the leaf area within an NDVI class of 0.8 – 0.9.
- A large proportion of early state psyllid-transmitted CLso-infected plants could be detected within two days by searching for anomalously high reflectance in the 570-650 nm in Innovator cultivar and at nine days in the Russet-Burbank cultivar.
- Since the differences between infected and healthy plants persist across a wide range of wavelengths, there is a reasonable prospect that a moderately-priced multispectral sensor (rather than an expensive hyperspectral sensor) could be flown by a drone over a potato crop and used to detect individual plants with the disease at an early stage.

Recommendations

- The findings from this shadehouse study indicated that there is a basis for spectral sensing of CLso-infected plants in a commercial potato crop setting.
- The next step is to determine whether individual CLso infected potatoes can be detected using the spectral approaches outlined multispectral cameras mounted on drones.
- We provide an outline for testing the results of this shadehouse experiment in the field with a view to developing an operational algorithm.

1 Introduction

The bacteria *Candidatus* Liberibacter solanacearum (CLso) is associated with the zebra chip disease of potatoes (Pitman et al., 2011), an economically important disease that can cause yield losses of up to 60% (Pitman et al., 2011. CLso can be transmitted to a potato crop by the potato psyllid, *Bactericera cockerelli*. Alternatively, infected mother tubers can act as a source of the bacteria.

Foliar symptoms of plants affected by zebra chip vary widely, but include an upward rolling of the basal portion of young leaves, chlorosis, purple top, shortened internodes, small leaves, enlargement of the stems, swollen auxiliary buds, aerial tubers and early plant senescence (Pitman et al., 2011).

Plants with CLso transmitted via the mother tuber exhibit the following symptoms: (a) germination failure; (b) successful germination but a spindly growth habit; (c) germinate and grow a non-diseased plant, or d. germinate and grow a diseased plant (and subsequently infected daughter tubers) (Pitman et al., 2011).

The purpose of this project was to investigate whether hyperspectral imaging could assist in early detection of this disease in potato plants. Our objective was to determine whether there is a hyperspectral signature for (a) plants grown from CLso-infected tubers; and (b) plants infected with CLso via transmission by the potato psyllid.

2 Background

Hyperspectral imaging is a technique of spectral imaging that can be compared to standard RGB photography. A standard RGB camera captures an image where each pixel contains information on just three spectral bands — we think of them as colours: red, green and blue. By contrast, each pixel of a hyperspectral image image contains information on hundreds of spectral bands — they may be thought of as finely resolved colours, but it is more correct to think of them as different wavelength bands. They often extend beyond the visible region of the electromagnetic spectrum and into the near-infrared and shortwave infrared.

Generically, plant stress causes changes to the spectral reflectance of leaves. Factors such as nitrogen deficiency can reduce the abundance of chlorophyll and other pigments, leading to greater reflectivity in the visible region (Carter, 1993). Hyperspectral sensing has been used extensively in the detection of plant diseases (Lowe et al., 2017; Mishra et al., 2017) and recently for the detection of Potato Virus Y in seed potatoes (Polder et al., 2019) using deep learning algorithms. However, a literature search revealed no publications on the use of hyperspectral imaging for the detection of foliar symptoms of CLso in potatoes, although benchtop hyperspectral imaging was used to detect the presence of Zebra Chip symptoms in potato tubers (Zhao et al., 2018).

3 Objectives

1. Set up and test an imaging system to capture hyperspectral imagery of potted potato plants in a shade house;

2. Use the system to monitor the spectral reflectance of potatoes infected with CLso via infected mother tubers (Experiment 1) and potatoes infected with CLso via the potato psyllid (Experiment 2);

3. Process and analyse the hyperspectral imagery with a view to developing an operational methodology for an 'early warning' system to be used in the field.

4 Methods

4.1 Growth of experimental plants and infection with CLso.

A detailed description of the preparation of the test plants and infection is provided in Vereijssen et al. (2019). However, a brief description of the experimental set-up is provided below.

4.1.1 Experiment 1. Investigation of the hyperspectral signature of potatoes infected with CLso via the infected mother tubers

Ten tubers of CLso-infected potato cultivar Russet-Burbank were germinated and grown in 4 L plastic pots together with ten identical but uninfected tubers as control specimens. They were planted on 23 October 2018 and placed in the shadehouse for hyperspectral imaging on 21 November 2018.

4.1.2 Experiment 2. Investigation of the hyperspectral signature of potatoes infected with CLso via the potato psyllid

Twenty tubers each of potato cultivars Russet-Burbank and Innovator were tested for presence of CLso via qPCR (Beard & Scott, 2013). All tested negative for CLso (data not presented).

On 19 October 2018, each tuber was planted 10 cm deep in a 4 L plastic pot in standard non-sterile potting mix filled 4 cm from the top at Plant & Food Research, Lincoln. Pots were moved to a shade house, where a tray was placed underneath each pot to act as a water reservoir and to assist even watering between pots. Tubers were watered thoroughly after planting and then once or twice weekly depending on their requirements.

On 23 January, nine weeks after planting, one leaf on 10 plants of each cultivar were exposed to CLso-positive *B. cockerelli*. The adding of the psyllids was delayed by 10-14 days because of non-availability of the hyperspectral camera. A mesh organza bag (Manufacturer MegaView Science) was placed over a leaf of a plant, and vial containing 5 psyllids was carefully placed in the bag. The psyllids were on the plant for 2 weeks, and

during this time the potato plants were scanned with a hyperspectral camera. The leaf with the organza bag was removed from the plant on 5 February 2019. Then, a tuber sample of each plant was tested for presence of CLso using qPCR according to Beard and Scott (2013). All plants within the control treatment tested negative for CLso, and all but two of the plants in the infected treatment tested positive. The two plants where infection was attempted but failed were replicates 'D3' and 'D5' from the ten Innovator cultivar replicates and the spectral information was removed from subsequent statistical analysis.

4.2 Hyperspectral Imaging

We used a Nano Hyperspec hyperspectral camera (Headwall Photonics, MA, USA). This is a line scanning camera with a 'push-broom' action, meaning that a single image consists of a spatial line of pixels in the x direction, but only 1 pixel in the y direction. However, each of the pixels within that single line contains data points for each spectral band. For this camera, there are 640 pixels in the x-direction, 1 pixel in the y-direction and 274 different spectral bands, ranging from 398 nm to 1004 nm. This spectral range encompasses the visible region (400 nm – 750 nm) and the near-infrared region (750 nm – 1000 nm). Accordingly, such a hyperspectral camera is known as a VIS-NIR camera.

To collect images of the potted potato plants, we designed and fabricated a gantry camera slider (Figure 1), that allowed the camera to be moved above the plants in the y-direction at a constant rate. The velocity of this motion was set according to the incident radiation and the corresponding exposure requirements of the camera. Eight hundred separate images (or lines) of data were collected over the travel distance of the camera slider (which moves in the y direction) resulting in a hyperspectral 'cube' of data with the following dimensions: 640 pixels width × 800 pixels height × 274 spectral bands.

In Experiment 1 (the infected tuber experiment), each plant was imaged a total of five times at 31, 35, 38, 48 and 52 days after planting. In Experiment 2 (the psyllid-infection experiment) each plant was imaged a total of 10 times between 95 and 150 days following planting (and ranged between one day before and 54 days after infection with CLso via the psyllid vector). The experimental timeline is provided in Table 1.

Figure 1 A Headwall Photonics Nano hyperspectral camera mounted on automated gantry system. The camera slides along the rail at a velocity proportional to the amount of incident light. Potato plants were scanned in pairs. A single scan of the plants collected a hyperspectral 'cube' consisting of 800 lines of 640 pixels × 274 spectral bands. The card lying between the plants acts as a reference to convert radiance into reflectance.

Table 1 Experimental details and timeline

Experiment 1 - Comparing plants infected with CLso via CLso-infected mother tubers

Varieties tested: Russet-Burbank

Number of replicates:	10 in each of the infected and control treatments
Day of planting	23/10/2018

Hyperspectral Image Acquisition Dates

Sampling #	Date	Days Since Planting
1	23/11/2018	31
2	27/11/2018	35
3	30/11/2018	38
4	10/12/2018	48
5	14/12/2018	52

Experiment 2 - Comparing plants infected with CLso via the potato psyllid

Varieties tested: Russet-Burbank, Innovator

Number of replicates	10 in each of the infected and control treatments for each cultivar (40 Plants total)
Day of planting	19/10/2018
Day of CLso infection via psyllid	23/01/2019

Hyperspectral Image Acquisition Dates

Sampling #	Date	Days Since Planting	Days Since Infection
1	22/01/2019	95	-1
2	25/01/2019	98	2
3	1/02/2019	105	9
4	7/02/2019	111	15
5	12/02/2019	116	20
6	20/02/2019	124	28
7	27/02/2019	131	35
8	4/03/2019	136	40
9	11/03/2019	143	47
10	18/03/2019	150	54

4.3 Image Processing

4.3.1 Conversion of raw data to radiance

The hyperspectral camera collects raw data as uncalibrated digital numbers. These were converted to a physical radiance value with units of mW $[cm^2.sr.\mu m]^{-1}$. This was done using the camera's post-processing software SpectralView version 5.5.1 (Headwall Photonics, MA, USA). SpectralView uses a camera-specific factory calibration for each pixel and the manufacturer's recommended dark calibration, which was conducted at each sampling occasion in the shadehouse. Using this software, we created a radiance image for each raw image. Each radiance image had identical dimensions to its corresponding raw image (640 pixels width × 800 pixels height × 274 spectral bands).

4.3.2 Conversion of radiance data to reflectance

Each image contained two potato plants in pots together with a calibration card in the middle. The calibration card had three panels with standardised reflectance of 1%, 18% and 99% for the black, grey and white panels, respectively (Figure 2). A Python software program was developed to iterate through the radiance images and allowed the user to draw a four-sided polygon with the mouse over the area of the image that corresponded to the white, grey and black panels. From the average reflectance of the black and grey panels, a two-point linear transform function was calculated, and then used to convert each radiance image to a reflectance image (where each pixel is a reflected radiance as a proportion of incident (incoming) radiance at each spectral band.

4.3.3 Detection of Plant Area

To distinguish living leaf tissue area from non-plant material or dead tissue, we used the spectral vegetation index Normalised Difference Vegetation Index (NDVI) (Tucker, 1979). The formula for NDVI is:

NDVI = (NIR – Red) / (NIR + Red)

We defined red as the average reflectance over the spectral range from 630 to 690 nm and NIR as the average reflectance over the spectral range from 770 nm to 900 nm.

NDVI values were calculated for each image and used as a masking variable to detect living plant area. For experiment 1, a NDVI threshold of 0.5 was used as a criterion to detect plant tissue. Lower NDVI threshold values led to confusion between the plant and non-plant areas of the image.

4.3.4 Processing of hyperspectral reflectance data for each plant

For each pixel of plant material in each image, the following metrics were calculated: (a) reflectance within each spectral band; (b) average reflectance across 20 nm spectral ranges; (c) a variety of spectral vegetation indices in addition to NDVI. We then collected statistics — mean, median, standard deviation, minimum, maximum and 5^{th}, 10^{th}, 25^{th} percentiles — on each of these metrics across each plant. Only statistics for NDVI, the

single band reflectance and the 20 nm band averages were found to be useful for CLso detection and other metrics are not discussed further.

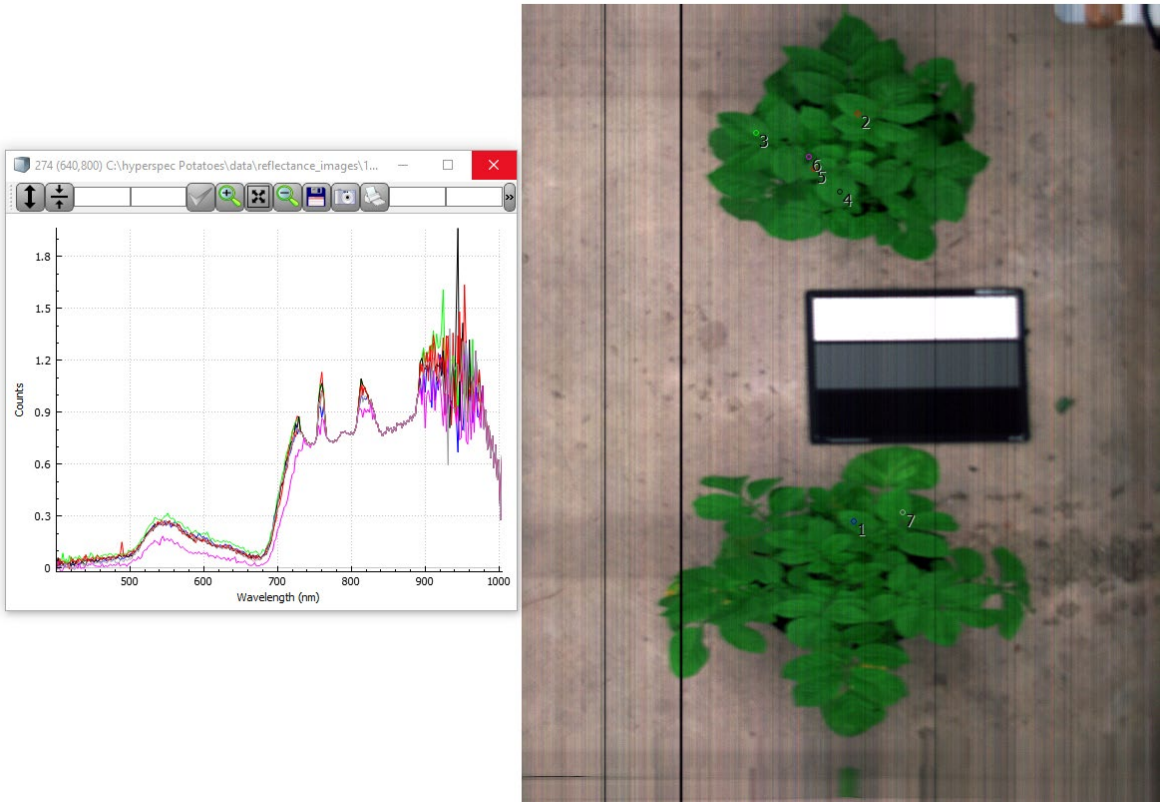

Figure 2 The right panel shows an example hyperspectral reflectance image of an infected plant (top) and a healthy plant (bottom). The radiance is converted to reflectance by imposing a linear transform over the entire image so that reference card in the centre gives reflectance value of 18% (grey panel) and 1% (black panel). The left panel shows the reflectance spectra for selected points on the image.

5 Results

5.1 Plant Growth

The results of the plant growth were reported in Vereijssen et al. (2019). Briefly, in Experiment 1 plants remained green and healthy over the duration of the experiment. However, plants emerging from infected tubers tended to be smaller but greener. Plants emerging from the uninfected tubers tended to be larger but had visual signs of senescence.

In Experiment 2, heat conditions in the shade house caused plant stress and resulted in senescence across all plants, which complicated the hyperspectral analysis.

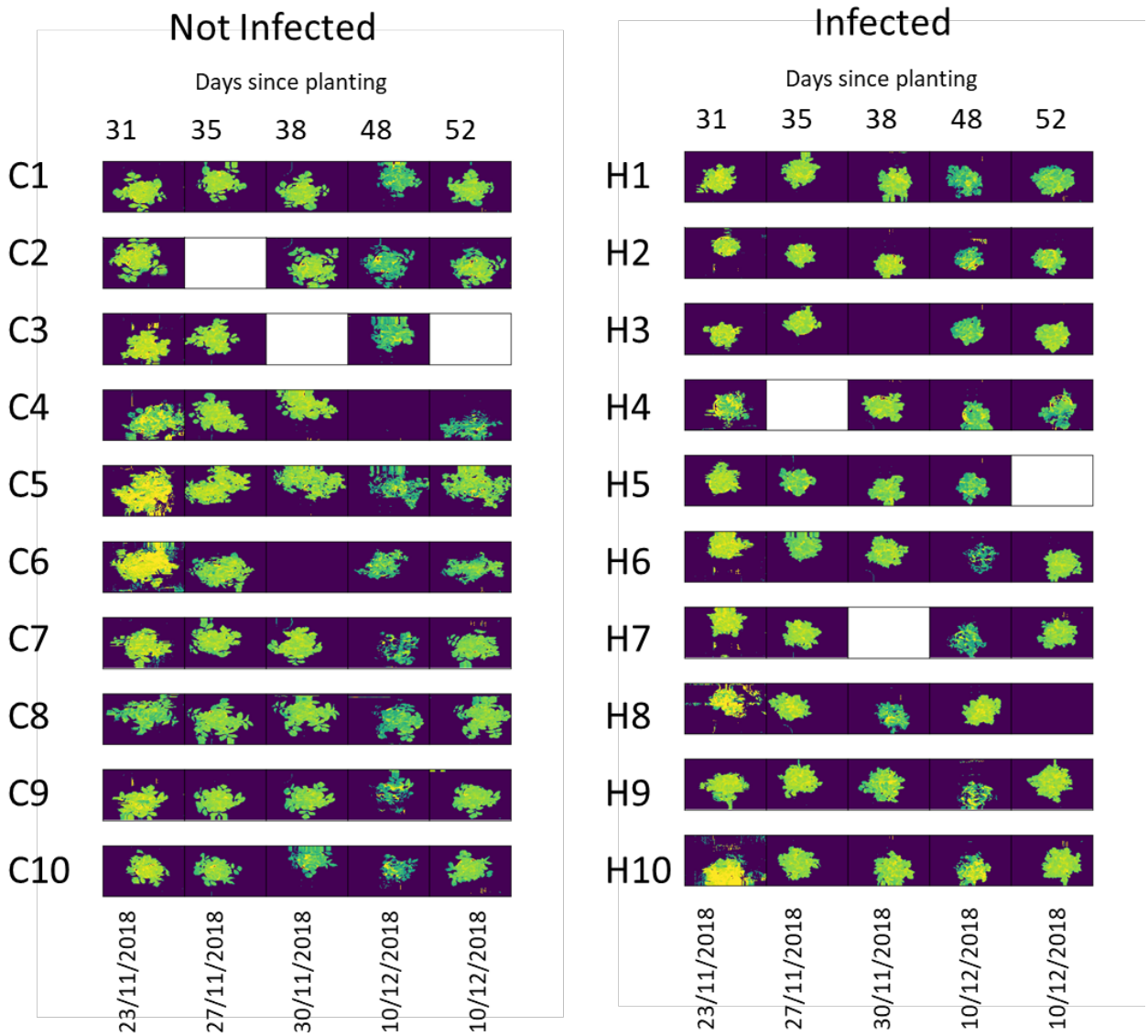

Figure 3 NDVI images of 10 infected and 10 non-infected plants from Experiment 1. H1-C10 refer to individual plant idenitification numbers.

5.2 Experiment 1 – Comparing Clso-Infected and Healthy Tubers

5.2.1 Image collection

A total of 258 hyperspectral images were collected: 50 were collected during Experiment 1 on 5 separate sampling occasions; 208 were collected during Experiment 2 on 10 separate sampling occasions. The NDVI-masked images for Experiment 1 are shown in Figure 3 and for Experiment 2 in Figure 10 through Figure 13 in the Appendix.

Some problems were encountered with heat in the shade house deforming the plastic components of the gantry leading to uneven motion of the camera and low quality imagery. This led to the rejection of five images in Experiment 1.

5.2.2 Green area of individual plants

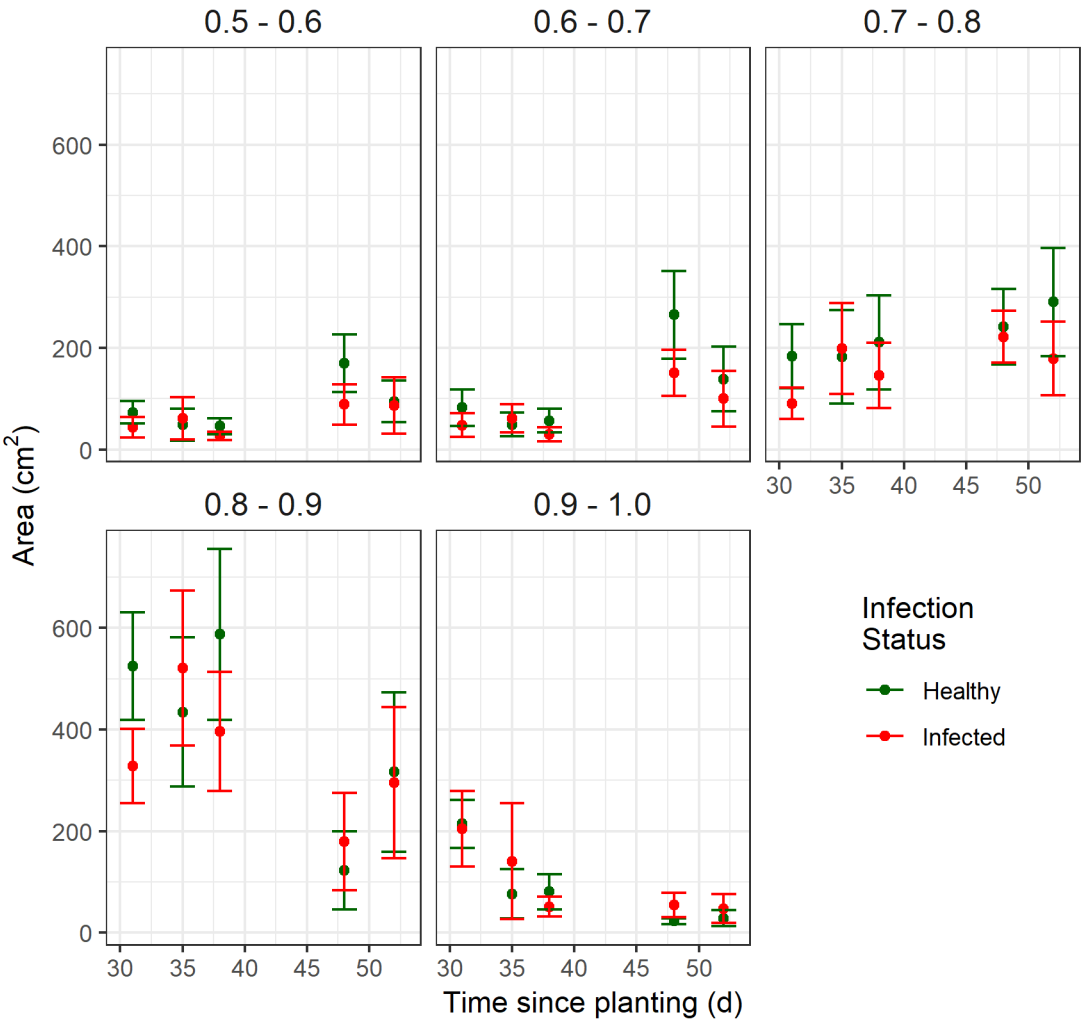

Figure 4 Leaf area in five different NDVI classes in Experiment 1 – comparison of infected and healthy tubers. Panel labels indicate the range of NDVI. Error bars denote 95% confidence intervals

Overall the variation in total green area was not significantly different dur to a large amount of variability among replicates (data not shown). This may be explained by the

opposing effects of smaller plant size in the infected plants and a greater level of senescence in the uninfected plants.

However, when the data was separated into different classes of greenness (measured here by NDVI calculated on a per-pixel basis), we could distinguish between healthy and infected tubers at day 31 within the NDVI class 0.8 to 0.9 (Figure 4).

5.2.3 Spectra at different sampling dates during Experiment 1

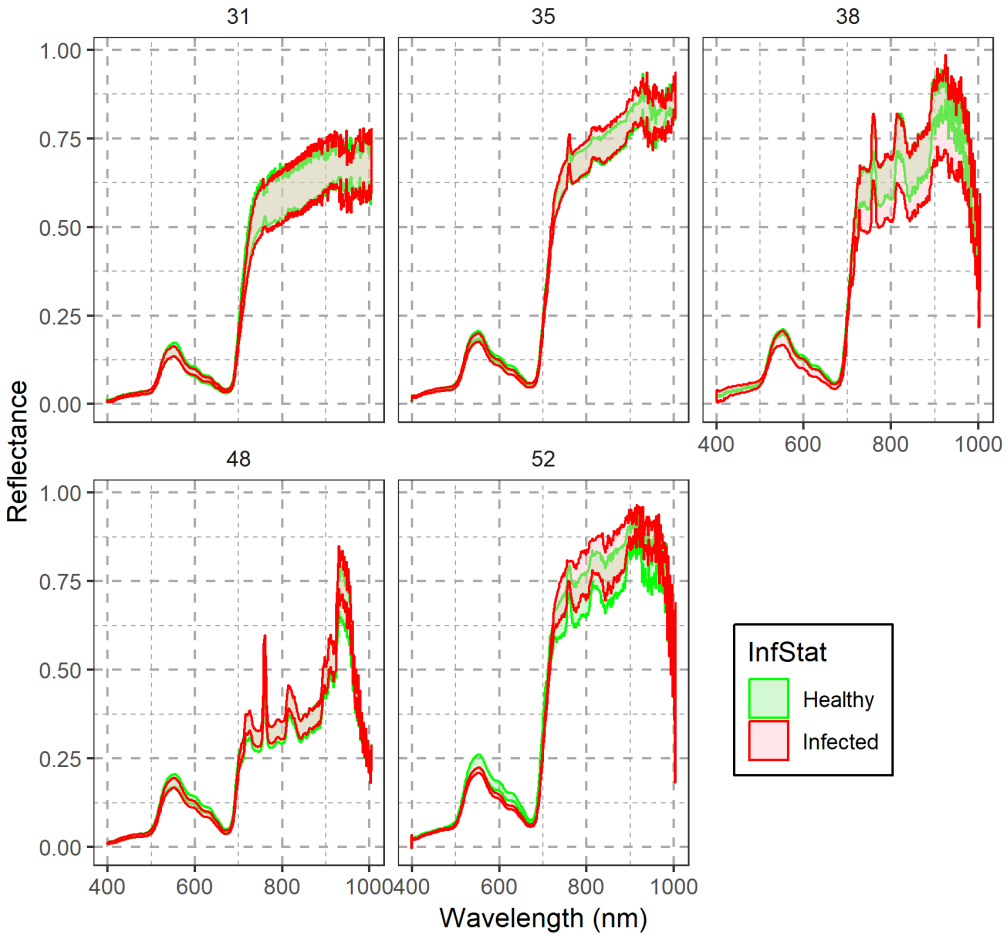

Figure 5. 90% Confidence intervals of spectral reflectance for potato plants with healthy and infected tubers at five time points. Numbers at top of panel indicate days since planting.

Overall, the spectra showed characteristic patterns consistent with the literature (for example, Carter and Knapp (2001)) (Figure 5). Reflectance is generally lower and less variable in the visible region (400-740 nm) with an obvious local peak in the wavelengths corresponding to green reflectance (around 550 nm). The steep increase in reflectance from ~680 nm to ~750 is known as the "red edge" and its position and shape contain information regarding chlorophyll content, biomass and hydric status (Filella and Penuelas, 1994). Reflectance at higher wavelengths (750 to 1000 nm, known as the "Near Infrared Region or NIR"). Reflectance in this region was more variable among replicates, and increased less sharply and less smoothly with increasing wavelength then reflectance in

the "red edge" region. The signal-to-noise ratio for the camera's sensor decreases markedly above 900 nm and the usefulness of reflectance values above 900 nm is limited.

The spectra differed markedly over the course of Experiment 1, but were remarkably similar between treatments. This suggests that inspection of the spectra alone would not provide a satisfactory basis for detection of plants emerging from infected tuber. Our analysis of spectral vegetation indices, in addition to NDVI, did not reveal obvious differences between infected and uninfected plants.

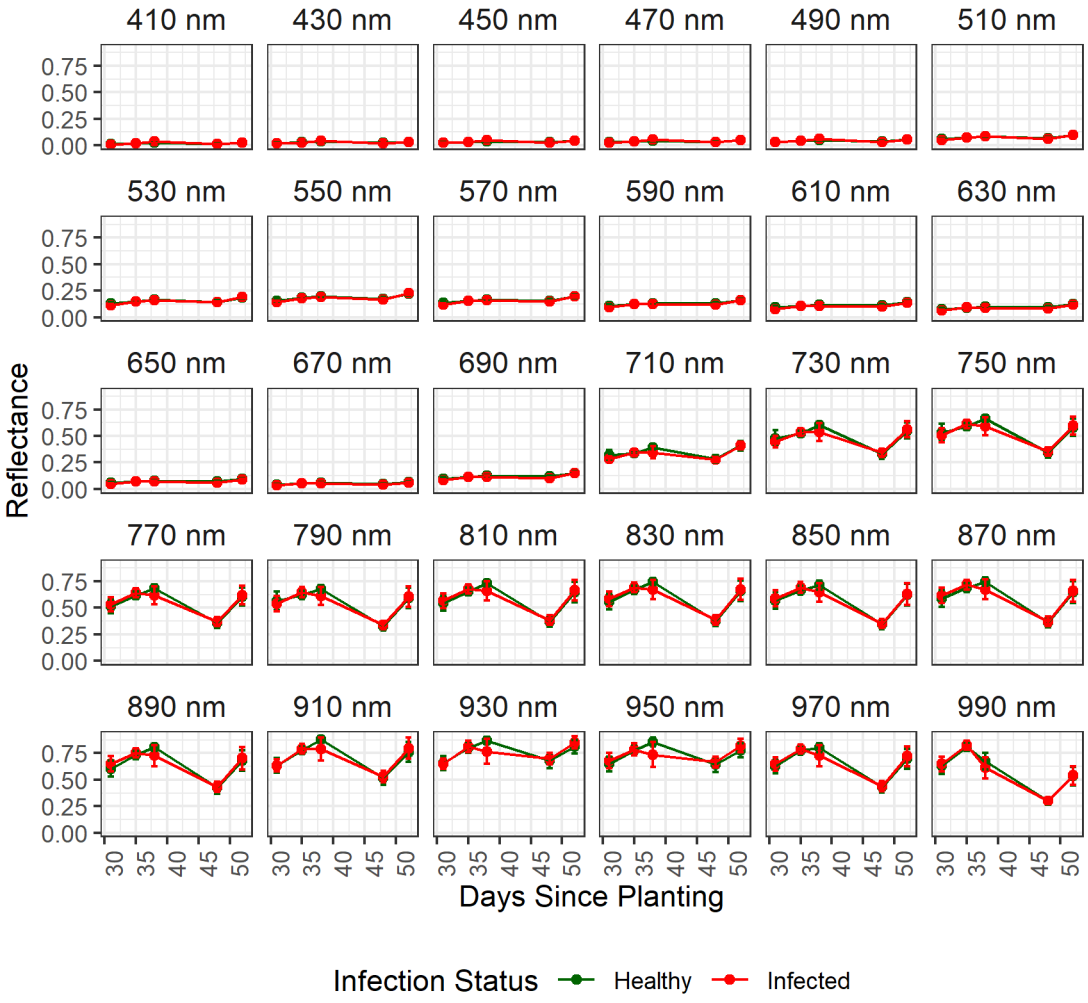

Figure 6. Mean reflectance of plants in Experiment 1 within different spectral bands of 20 nm width centred on the wavelength in panel label. Error bars represent 95% confidence intervals.

The similarity between healthy and infected plants is underscored in Figure 6 where significant differences at any wavelength region were not apparent.

We undertook three other lines of analysis to form a detection algorithm for infected tubers. First, we calculated a large number of spectral vegetation indices (Table 1). Second, we tried differentiation of the red edge – an approach suggested by Filella and Penuelas

(1994). Finally, we tried a simple machine-learning approach known as Support Vector Machines (SVM). None of these techniques were successful in reliably distinguishing between infected and non-infected plants at an early stage.

In summary, we did not find a distinct hyperspectral signature characteristic of plants grown from CLso-infected tubers. However, the camera was useful in allowing us to calculate NDVI – a more reliable measurement of greenness than RGB imagery and comparing the plant area within an NDVI range of 0.8-0.9.

5.3 Experiment 2 — Infected Tubers

5.3.1 Amount of Green Area

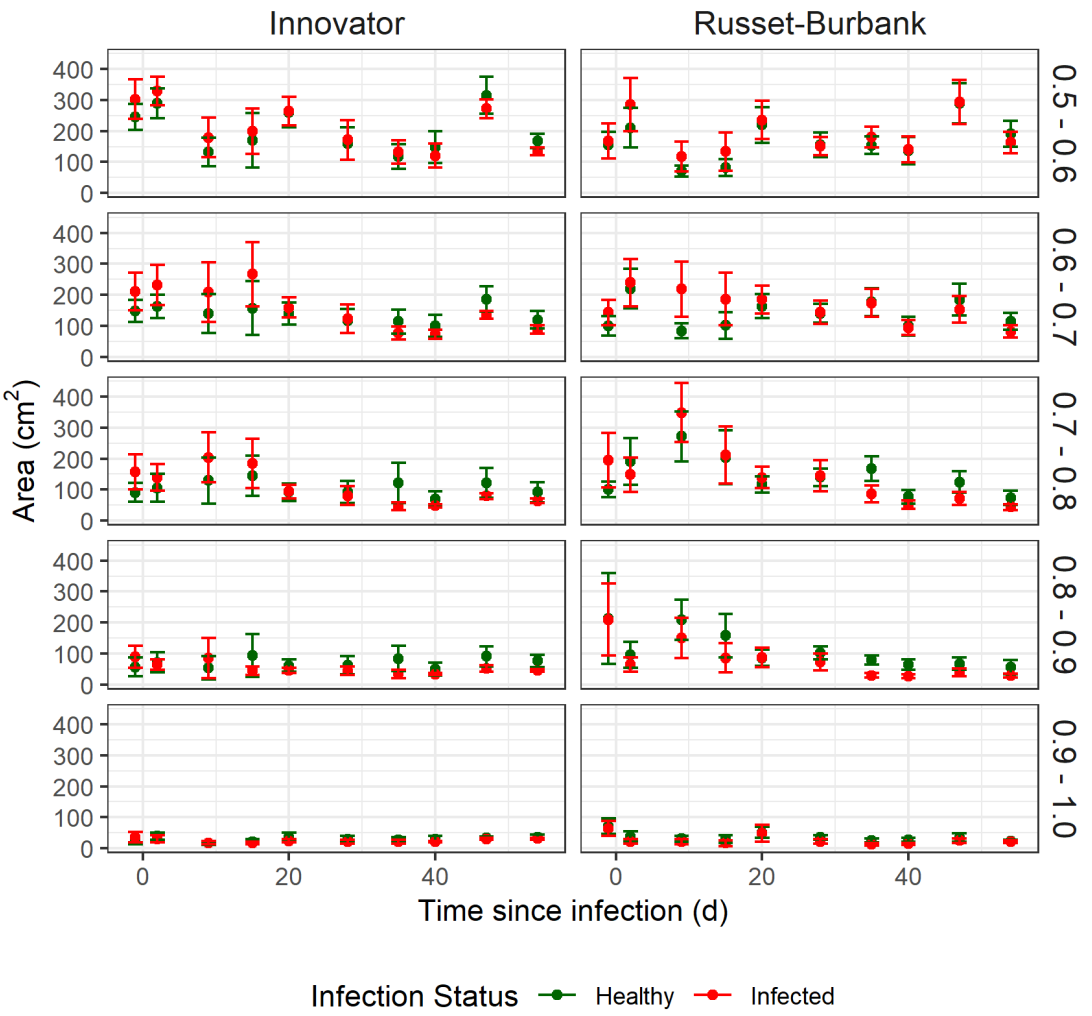

Figure 7 Green leaf area Median (± 90% confidence interval) in five different NDVI classes and two different cultivars of potato in Experiment 2 (Psyllid-infected Trial). Panel labels on the right-hand side indicate the lower and upper bounds of the NDVI class.

The quantification of the green area within different NDVI classes was not significantly different between infected and healthy plants, and accordingly would not form a reliable basis for the detection of plants infected with CLso via the potato psyllid vector. Large overlapping confidence intervals during the early stages of infection would preclude us using a simple green-area as an early warning basis for the disease (Figure 7).

At later stages (>30 days) in the experiment, the presence of non-overlapping error bars indicated that separation based on the amount green area within the 0.7-0.8 and 0.8-0.9 NDVI ranges. However, since the goal of this research was to seek an 'early warning' detection algorithm, we did not further pursue this possibility.

5.3.2 Spectral differences between infected and uninfected plants in first 20 days since infection

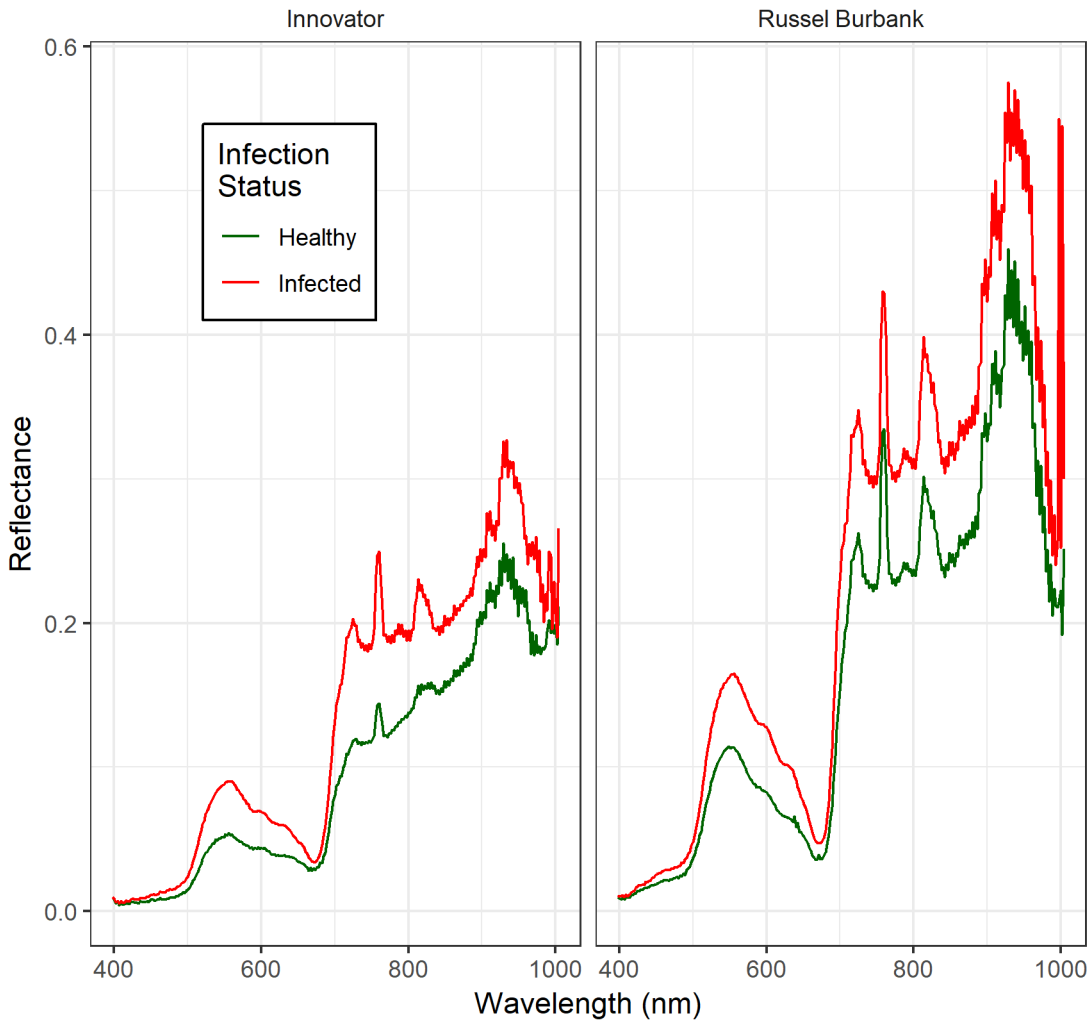

Figure 8 Median Spectra over all wavelengths for Experiment 2 from before infection until 20 days after infection (Comparing Psyllid-infected plants).

The median spectra over the first 20 days and over all replicates in Experiment 2 indicated that infected plants generally had greater levels of reflectance across the entire spectral range. The slope of the "red-edge" region was greater in the infected potatoes than the healthy plants. Substantial differences between the two cultivars also occurred. The Russet-Burbank cultivar was almost twice as reflective as the Innovator cultivar. Spectral features in the NIR were more pronounced in the Russet-Burbank plants.

5.3.3 Range of spectra among replicates during first 20 days since infection

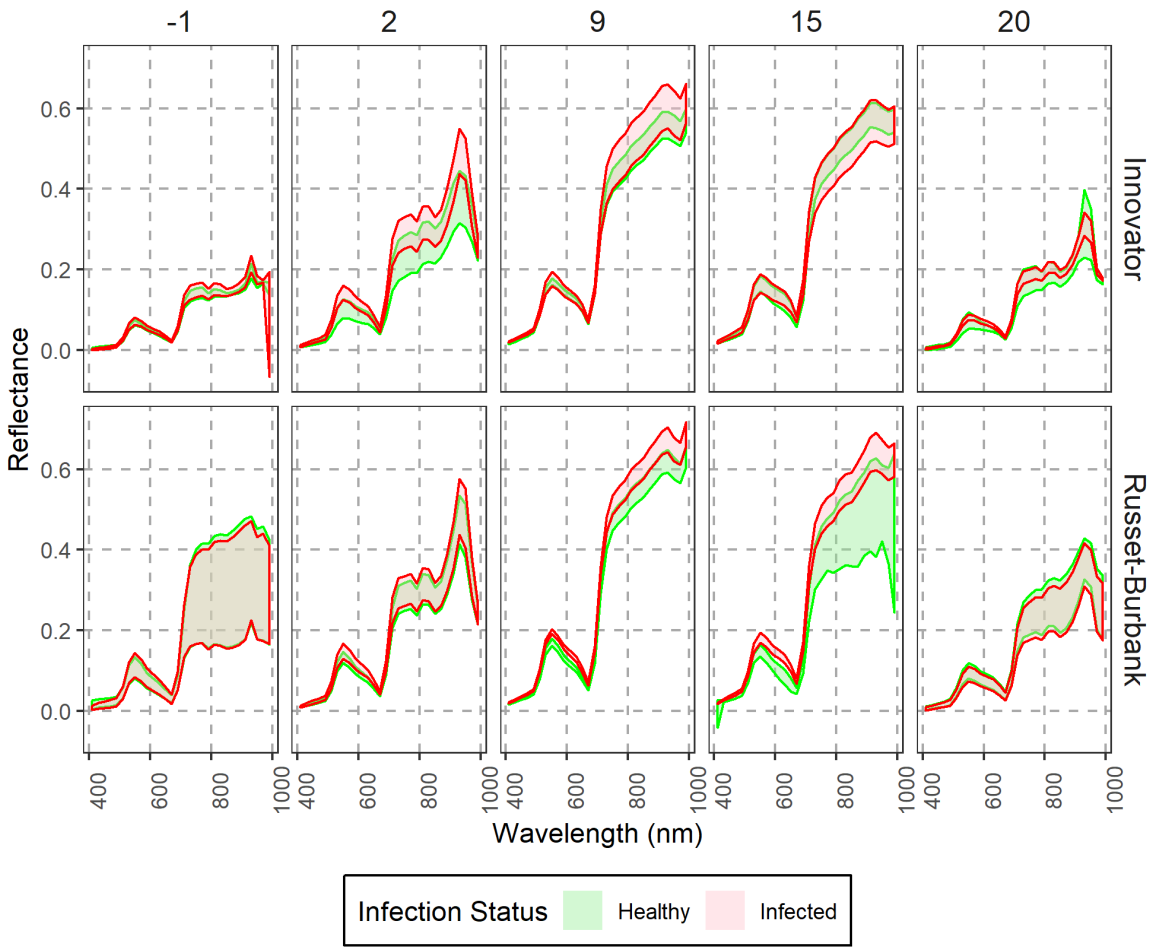

Figure 9. Reflectance spectra of potato plants at five time points since psyllid-mediated CLso infection. The ribbons show the upper and lower bounds of the 90% confidence interval. The numbers at the top of the panels denote the number of days since the plants were exposed to the disease.

We observed the evolution of small but systematic differences in the spectra between infected and healthy plants (Figure 9). These differences evolved over the first 20 days, where for both varieties spectral were indistinguishable before infection. Before infection (Day -1) the spectra overlapped moderately closely for both varieties. Over the ensuing 10 days, the reflectance of plants increased markedly, particularly in the NIR. However, the rate of increase in reflectance was greater for the infected plants and by day 2 the confidence bands for healthy and infected plants had almost separated for the Innovator cultivar in the visible region at 550 nm.

By day 9 a full separation of the confidence bands had occurred across the regions 530-610 nm in the Russet-Burbank cultivar. A partial separation also occurred in the range 730-910 nm in the Russet-Burbank cultivar on this day.

By day 15, the reflectance spectra almost fully overlapped for Innovator and was partially overlapping for Russet-Burbank cultivars.

By day 20, the plants were undergoing heat-induced senescence, spectral reflectance was lower than the previous three measurements and the confidence bands for healthy and infected treatments were largely overlapping.

While the separation of the infected and non-infected confidence bands is only partial, they are consistent with the idea that plant stress elicits greater reflectance in the visible region (Carter, 1993). Since this greater reflectance is systematically associated with infected plants, this seems a reasonable basis to form an early screening system for CLso in the field with an inexpensive camera.

6 Conclusions

Hyperspectral imaging of CLso-infected and uninfected potatoes revealed two possible approaches for early-stage detection of CLso symptoms.

- Each approach required, first, that the living tissue of plants be recognised and separated from the background by converting the hyperspectral imagery to an NDVI image and only including pixels where NDVI exceeded a threshold value of 0.5.
- At 30 days following planting, plants infected with CLso via infected mother tubers had significantly lower leaf area that fell within the NDVI range 0.8 to 0.9 compared with uninfected plants.
- A large proportion of early state psyllid-transmitted CLso-infected plants could be detected within two days following infection (95 days after planting) by searching for anomalously high reflectance in the 570-650 nm in Innovator cultivar and at nine days (105 days following planting) in the Russet-Burbank cultivar.
- Since the differences between infected and healthy plants persist across a wide range of wavelengths, there is a reasonable prospect that a moderately-priced multispectral sensor (rather than an expensive hyperspectral sensor) could be flown by a drone over a potato crop and used to detect individual plants with the disease at an early stage.

7 Recommendations

The findings from this shadehouse study indicated that there is a basis for spectral sensing of CLso-infected plants in a commercial potato crop setting. The next step is to determine whether individual CLso-infected potatoes can be detected using these approaches in the context of commercial potato crop. We recommend the following approach:

- Using a multispectral sensor mounted on a multirotor drone obtain imagery from a potato crop that is known to contain both CLso-infected and healthy plants. Imagery should be acquired at several early time points during the growing season.
- A suitable multispectral sensor might be the popular MicaSense RedEdge MX (MicaSense Inc, Seattle, WA, USA), which acquires imagery in five spectral

bands: three visible (475 nm, 565 nm, 680 nm), the red edge (730) and NIR (840 nm). This retails for $5500 USD.

- Convert multispectral imagery to NDVI and attempt to use object-based image analysis software to segment individual plants into coherent objects.
- For each plant calculate the following metrics:
  - i The amount of leaf area (inferred from number of pixels) within five NDVI classes;
  - ii the median reflectance in the sensors green band.
- Investigate the statistics of these metrics and relate it to the known infection status of potato plants in the imaged area of the crop. The work conducted in this study indicates that: (a) plants infected via the mother tuber will have lower leaf area in the NDVI range 0.8 to 0.9, and (b) that plants infected via the potato psyllid will be more reflective in the 565 nm range. Individual plants that fall into the lower and higher quantiles for metrics (i) and (ii) above, respectively, should be tested for the presense of CLso infection.

8 Acknowledgements

Falk Kalamorz and Lisa Watkins grew the plants, managed the psyllid infection and prepared the shadehouse as a staging site for the experiment. Kishor Kumar constructed and programmed the gantry camera slider system. Paul Peterson provided technical support with the testing of the camera and the gantry. John Hunt and Scott Graham collected the imagery on the fifteen sampling occasions for Experiment 1 and 2. We are grateful to Potatoes NZ for funding this research via an MPI Sustainable Farming Fund Project.

9 References

Carter, G.A., 1993. Responses of Leaf Spectral Reflectance to Plant Stress. American Journal of Botany 80, 239-243.

Carter, G.A., Knapp, A.K., 2001. Leaf optical properties in higher plants: linking spectral characteristics to stress and chlorophyll concentration. American Journal of Botany 88, 677-684.

Filella, I., Penuelas, J., 1994. The red edge position and shape as indicators of plant chlorophyll content, biomass and hydric status. International Journal of Remote Sensing 15, 1459-1470.

Lowe, A., Harrison, N., French, A.P., 2017. Hyperspectral image analysis techniques for the detection and classification of the early onset of plant disease and stress. Plant Methods 13, 80.

Mishra, P., Asaari, M.S.M., Herrero-Langreo, A., Lohumi, S., Diezma, B., Scheunders, P., 2017. Close range hyperspectral imaging of plants: A review. Biosystems Engineering 164, 49-67.

Pitman, A.R., Drayton, G.M., Kraberger, S.J., Genet, R.A., Scott, I.A.W., 2011. Tuber transmission of 'Candidatus Liberibacter solanacearum' and its association with zebra chip on potato in New Zealand. European Journal of Plant Pathology 129, 389-398.

Polder, G., Blok, P.M., de Villiers, H.A.C., van der Wolf, J.M., Kamp, J., 2019. Potato Virus Y Detection in Seed Potatoes Using Deep Learning on Hyperspectral Images. Frontiers in Plant Science 10.

Tucker, C.J., 1979. Red and photographic infrared linear combination for monitoring vegetation. Remote Sesning of the Environment 8, 127-150.

Vereijssen, J., George, M., Kalamorz, F., Dellow, S., Watkins, L., Addison, S., 2019. SFF Precision Agriculture in Seed Potatoes - Year 2 progress report. Plant and Food Research.

Zhao, Z., Prager, S.M., Cruzado, R.K., Liang, X., Cooper, W.R., Hu, G., Rashed, A., 2018. Characterizing Zebra Chip Symptom Severity and Identifying Spectral Signatures Associated with 'Candidatus Liberibacter solanacearum'-Infected Potato Tubers. American Journal of Potato Research 95, 584-596.

Appendix 1 –

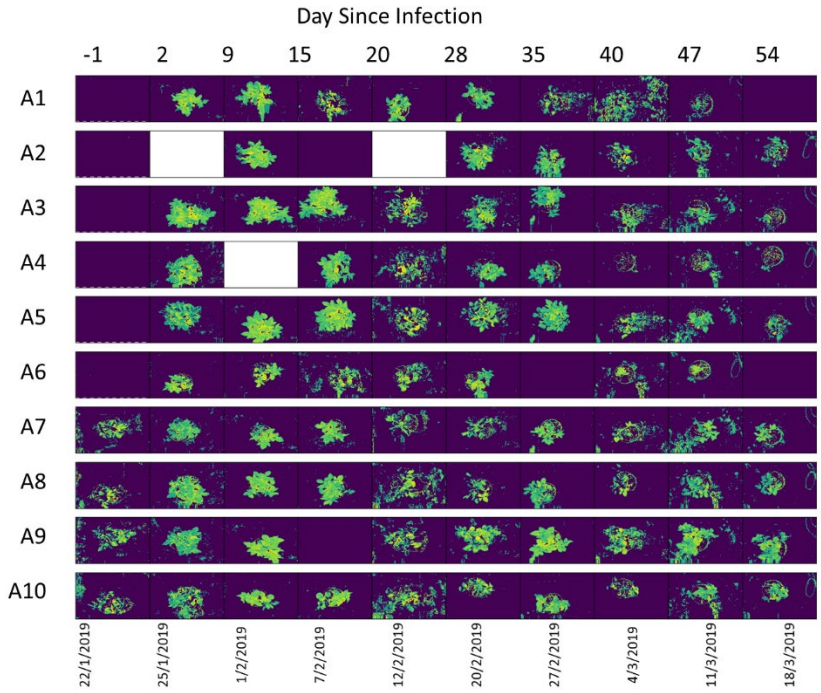

Figure 10 NDVI Images for Experiment 2 — Treatment A: Cultivar "Russet-Burbank" – Not Infected (control). Numbers at top of figure indicate days since infection.

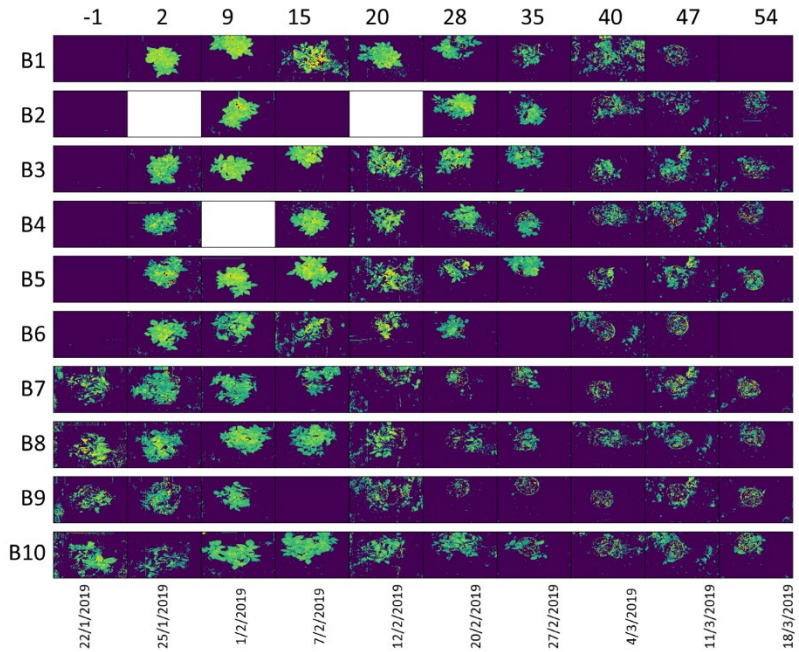

Figure 11 NDVI Images for Experiment 2 — Treatment B: Cultivar "Russet-Burbank" – Infected. Numbers at top of figure indicate days since infection.

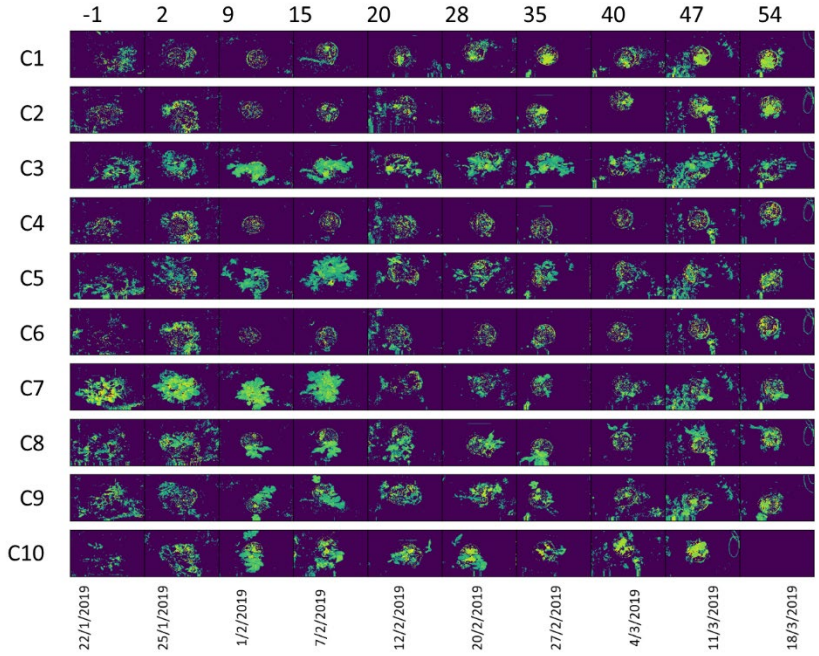

Figure 12 NDVI Images for Experiment 2 — Treatment D: Cultivar "Innovator" – Not Infected. Numbers at top of figure indicate days since infection.

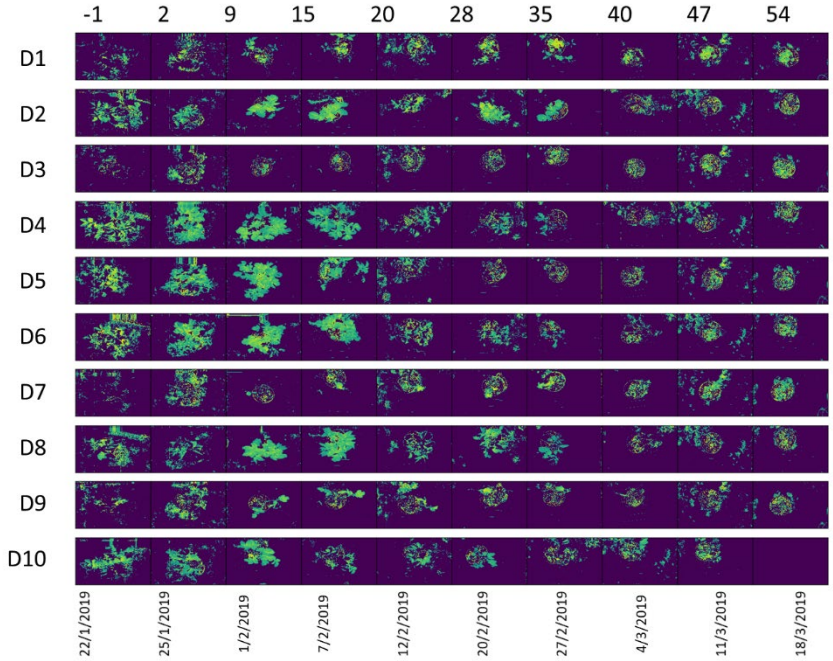

Figure 13 NDVI Images for Experiment 2 — Treatment D: Cultivar "Innovator" – Infected. Numbers at top of figure indicate days since infection.